Structural relaxations of phospholipids and water in planar membranes

C. Svanberg,[a] P. Berntsen, A. Johansson, T. Hedlund, E. Axén, and J. Swenson[b]
Department of Applied Physics, Chalmers University of Technology, SE-412 96 Göteborg, Sweden

(Received 15 August 2008; accepted 24 November 2008; published online 20 January 2009)

We have used dielectric spectroscopy and temperature modulated differential scanning calorimetry (TMDSC) to investigate the structural relaxation processes and phase transitions of water and lipids in multilamellar, planar phospholipids. At low hydration levels we observe the main structural relaxation related to the glass transition of the phospholipids. With increasing water content a more pronounced pretransition, attributed to a gel to ripple phase transition, is observed in the TMDSC data. In the proximity of this pretransition, a distinct change in the temperature dependence or alternatively a bifurcation into two processes is observed in the dielectric data. Around this temperature a crossover in the long-range ionic conductivity across the membranes is also observed, which is one of the key parameters for biological membranes. Thus, the major dynamical changes do not occur at the main, i.e., the gel to liquid structural phase transition, but at a pretransition that occurs roughly 20 K below the main transition. © *2009 American Institute of Physics*.
[DOI: 10.1063/1.3054141]

I. INTRODUCTION

At biological temperatures cell membranes are a fluid mosaic of lipids and proteins[1,2] that constantly undergoes architectural changes. A major component in biological membranes is phospholipids that possess a remarkable combination of fluidity and rigidity.[3] Phospholipids are amphiphilic molecules and hence both the interaction within the membrane, i.e., between the lipids, and with the surrounding water molecules are important. This is also the cause for the self-assembly of lipids into structures such as bilayer or micelles. However, the understanding of the structure of lipid membranes has progressed much further than the dynamics,[4] despite that the dynamics is crucial for many important biochemical processes, such as drug transport and protein activity.[1]

Experimentally the dynamics of phospholipids and the adjacent water has been probed using techniques such as NMR,[5] quasielastic neutron scattering (QENS),[6–8] dynamic light scattering,[9] and dielectric spectroscopy.[10–18] Computer simulations have also improved our understanding of the structure and dynamics at different hydration levels, temperatures, and phase configurations.[19,20] These studies have shown that the dynamics of hydrated lipid membranes includes several different types of processes, such as fast diffusion of water molecules, rotation of the lipid heads, segmental motion of the lipid tails, and two dimensional (2D) translational diffusion of lipids within the layers.[13,20] Moreover, the dynamics of the lipids is intimately coupled to the arrangements of the lipids in the membranes. At low temperatures the acyl chains tend to be all-*trans* resulting in a high degree of ordering of the tails, the so-called gel phase. This phase is commonly denoted L_β or $L_{\beta'}$ depending on if the lipid tails are perpendicular to the membrane surface or tilted.[21] At higher temperatures the configuration of the tails becomes more disordered, the so-called liquid or L_α-phase. This gel to liquid phase transition has direct impact, not only on the dynamics of the lipids, but also on the surrounding water molecules, and that results in a more disordered state of the surrounding water[22] and a deeper penetration of water molecules into the membrane.[20]

Water embedded in, or at the surfaces of, biomolecules are essential for the biological function, but the relation between the dynamics and the functionality is currently debated.[23] For phospholipids it has been shown that upon hydration the first few water molecules form an inner hydration layer that primarily interact with the phosphate groups of the lipid heads.[6,24] These water molecules can also act as water-bridges between different lipids[2] and the membrane perturbs the hydrogen bonded water-network up to some 5 Å from the surface. Reduced hydration leads to a decreased area per lipid and thicker lipid bilayers due to an enhanced bilayer-bilayer interaction.[25] Decreased hydration also drastically reduces the tendency of water to crystallize and hence a potential route to storage of biological material with retained chemical and physical integrity.[26] Moreover, important biological events, such as cell fusion, occur at low hydration levels.[25] Moderately hydrated lipid membranes[27] and other types of nano-confinement[28–31] have also been used to explore the currently debated properties of deeply supercooled water.[32]

A constituent part of many cell membranes is palmitoyl-oleoyl phosohatidylcholine (POPC). POPC is an asymmetric lipid belonging to the phosphatidylcholine family with 16 and 18 carbon atoms in the tails. Halfway down the long chain there is a double bond and unsaturated lipids generally give a more fluid-like behavior at room temperature and a lower liquid-gel transition temperature, T_m.[33] Therefore un-

[a]Present address: Innovation Center, Borealis AB, SE-444 86 Stenungsund, Sweden.
[b]Author to whom correspondence should be addressed. Electronic mail: jan.swenson@chalmers.se.

saturated lipids are an important component in biological membranes.[33] Experiments[21] and computer simulations[33] have shown that below T_m the tails of POPC are tilted, i.e., in a $L_{\beta'}$-phase. Above the chain melting temperature,[33] or at reduced water content,[25] the heads tend on average to be more oriented in the plane of the membrane. Recent experiments have also revealed that some phospholipids, including POPC, have a phase intermediate between the $L_{\beta'}$- and L_α-phases.[21] This, so-called ripple phase or $P_{\beta'}$, is characterized by a corrugated height profile with a wavelength of roughly 150 Å and a height of 50 Å.[21]

Despite the progress in our understanding of the structure and molecular mobility, the long-range collective dynamics of lipid membranes remains elusive[4] and scarcely investigated. There are also only a few reports on the glass transition in biological membranes,[26] and even fewer on the associated structural relaxation processes. A classical technique to probe glass transition related relaxations is dielectric spectroscopy, which has also been employed for lipid systems.[10–18] However, up to date the dielectric experiments have, with a few exceptions,[12,18] been performed on micelles in solutions where conductivity due to the surrounding solution dominates at low frequencies. This inhibits explorations of the very interesting slow dynamics. A route to circumvent this is to use planar membranes oriented perpendicular to the oscillating electrical field.[18] This approach enables investigations of slow dynamics and characterization of the supercooled and glassy regimes of phospholipids and water.

We here report on an investigation of the thermodynamics and molecular dynamics of planar multilamellar POPC membranes using dielectric spectroscopy and temperature modulated differential scanning calorimetry (TMDSC). By probing a broad frequency range we can identify the main relaxation processes of the lipids and water in the scarcely investigated supercooled regime. Furthermore, we investigate the dynamical changes across the gel-liquid phase transition and its effects on the ionic conductivity through the membranes.

II. EXPERIMENTAL

A. Materials

Following the approach described in Ref. 34 10 mg 1-palmitoyl-2-oleoyl-sn-glycero-3-phosphocholine (POPC, Avanti polar lipids) were dissolved in roughly 0.5 ml of isopropanol. The solutions were then spread on cleaned brass electrodes for the dielectric measurements. To anneal defects and to get a better alignment of the lipids, the membranes were tempered around the gel-fluid transition temperature. To remove residual solvent, the samples were placed under vacuum for 2–3 h. We have investigated samples exposed to three different humidities, which gives different amounts of water that are intercalated between the lipid layers. Samples hydrated in desiccators with Milli-Q water saturated with KCl and NaCl give 84% and 75% relative humidities (rhs), respectively. Phospholipids are known to spontaneous hydrate and hence a base level of water is present already at room humidity. For POPC the spontaneous hydration level is n_w=5 water molecules/POPC molecule[2,35] and the sample equilibrated at room humidity (typically 45% rh during the experiments) is denoted n_5. The uptake of water for the samples exposed to higher humidities was stabilized within a few days. For 84% and 75% rhs Binder has determined the hydration levels to approximately 10 and 8 water molecules/lipid, respectively,[36] and the samples will be denoted n_{10} and n_8.

B. Temperature modulated DSC measurements

The TMDSC experiments were performed using a TA Q1000 thermal analyzer. This technique is an extension of conventional DSC where a sinusoidal wave modulation is superpositioned on a linear temperature ramp, see, e.g., Ref. 37. This enables a separation of thermal events and transitions into "kinetic" and "heat capacity" responses of the measured sample.

Hermetically sealed pans were used for the samples and with an empty pan as reference. The TMDSC experiments were performed in a heat only temperature-modulation procedure starting at 100 K and then heated to 363 K with a ramp rate of 5 K/min and a temperature modulation of ± 0.8 K every 60 s.

C. Dielectric measurements

The experiments were performed using a high resolution dielectric spectrometer (Novocontrol, Alpha) from 130 up to 360 K in steps of 2 K. Prior to the dielectric experiments the samples were quenched down to 115 K by submerging them into a liquid nitrogen bath in order to avoid crystallization of the water. For each hydration level, the experiments were conducted on two different samples, prepared under identical conditions but with sample geometries optimized for high (10^6–10^9 Hz) and low frequency (10^{-2}–10^7 Hz) measurements. In the data analysis the high and low frequency data were merged into one set of data. The exact thickness of each sample is not known and at the phase transition the thickness of the POPC-layers can change. Therefore we will refrain from discussing the amplitudes of the processes.

III. RESULTS

A. Thermal transitions with TMDSC

With TMDSC we are able to separate the reversing and nonreversing heat flows. The reversing component is related to the sample's heat capacity, which means that a glass transition event is detected in the reversing heat flow. On the other hand, processes such as enthalpic relaxation, crystallization, and decomposition are resolved into the nonreversing heat flow.[37] For clarity we show only the total heat flow in Fig. 1 which displays the main features also seen in the reversing heat flow for these hydrated lipid membranes.

Three main features can be found in Fig. 1 for all hydration levels. Around 230 K all hydration levels exhibit an endothermic feature we denote, T_h, that probably arises from the onset of motions of the lipid head groups which requires that the H-bonds of the interfacial water molecules are broken.[2,38]

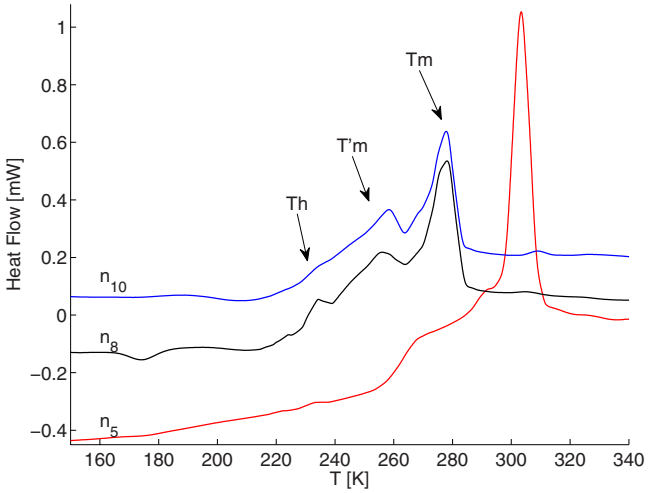

FIG. 1. (Color online) Total heat flow for the TMDSC heating experiment of hydrated POPC multibilayers, $n_{\text{water/lipid}}$: n_{10}, n_8, and n_5-samples. The data are vertically shifted for clarity.

The highest heat flow is observed for the endothermic process that occurs around 300 K. This peak is identified as the main transition, T_m, of the lipid membranes, i.e., the gel-liquid transition.[22] The main transition is typically hydration dependent in phospholipids with a melting point that takes place at a higher temperature when the hydration level goes down, as seen in Fig. 1 and presented in Table I.

Between T_h and the main transition, T_m, there is a feature at all hydration levels we call T'_m. For the two higher hydration levels T'_m is interpreted to arise from an interconversion of two different gel phases that takes place at the so-called gel to ripple pretransition.[21] For the low hydration level n_5 T'_m has the typical steplike feature of a glass transition, whereas it is more like a peak (typical for a first order thermodynamic phase transition) for n_8 and n_{10}. All the obtained transition temperatures are given in Table I.

The reason for that T'_m seems to have a slightly different physical origin for the lowest hydration level, compared to the two higher hydration levels, is likely that the ripple phase is not very pronounced at this low hydration level. Rather, for the n_5 sample T'_m is associated with a highly cooperative transition with a main dielectric relaxation time that approaches 100 s (typically seen for a true glass transition, as discussed in Sec. IV D below). For the hydrated samples n_8 and n_{10} the interactions between the hydration water and the lipids result in a more gradual melting endotherm, seen already from ~220 K in the total heat flow signal in Fig. 1. With less water in the system there is less energy interaction between the water and the lipids, which in turn gives more distinct thermal events. Lipid related features occur also at slightly higher temperatures at low hydration levels as more heat is needed to induce the thermal transitions in a low hydrated lipid system as n_5, particularly in the case of the main order-disorder transition at T_m. One should further note that the onset of lipid head motions around 230 K also gives a glass-transition-like feature. However, this transition is not a transition for the whole system, but should rather be considered as an onset of a more local secondary process, in analogy with β-relaxations in glasses. This interpretation is also supported by our dielectric results, as shown below.

TABLE I. Thermal transition temperatures for hydrated POPC multibilayers with $n_{\text{water/lipid}}$. T_h; head group, T'_m; pretransition, and T_m; main transition.

Hydration	T_h	T'_m	T_m (K)
n_5	233	263	303
n_8	234	255	278
n_{10}	234	258	278

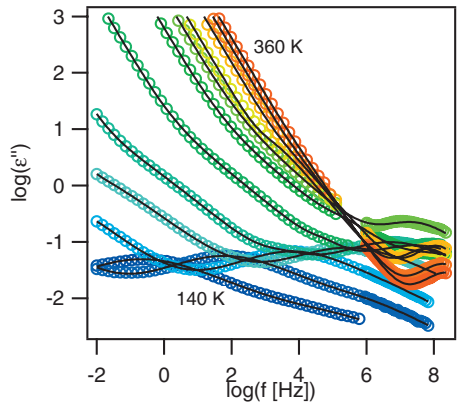

FIG. 2. (Color) Imaginary part of the permittivity, $\varepsilon''(\omega)$, for the n_8-sample at temperatures from 140 to 360 K in steps of 20 K from bottom to top. The full lines are the curve fits to the data.

B. Dielectric experiments

Figure 2 shows the imaginary part of the permittivity for the n_8 sample for selected temperatures. To describe the experimental data we use a term for the ionic contribution and a sum of the function proposed by Bergman,[39]

$$\varepsilon''(\omega) = \frac{A\sigma}{\omega} + \sum \frac{\varepsilon''_p}{\frac{(1-|a-b|)}{a+b}\left[b(\omega/\omega_p)^{-a} + a(\omega/\omega_p)^{b}\right] + |a-b|}. \quad (1)$$

Here ω_p is the peak relaxation frequency and a and b are the shape parameters. A in Eq. (1) incorporates the factors for the geometrical shape of the sample, such as thickness and area. At high temperatures the ionic conductivity dominates and therefore the ionic conductivity is analyzed first and subsequently the high frequency data in order to accurately describe the dynamical processes.

Figure 3 shows the temperature dependence of the peak relaxations obtained from the curve fit superimposed onto an intensity plot of the experimental data of the n_8 sample. At the low temperatures we observe a broad relaxation peak with a shoulder at high frequencies. The shoulder is most likely due to a weak faster process that is partly submerged, and we will denote it as process 3. Due to the difficulty to independently determine the peak position we use the same value for both n_8 and n_{10}. The main process (denoted 2) is

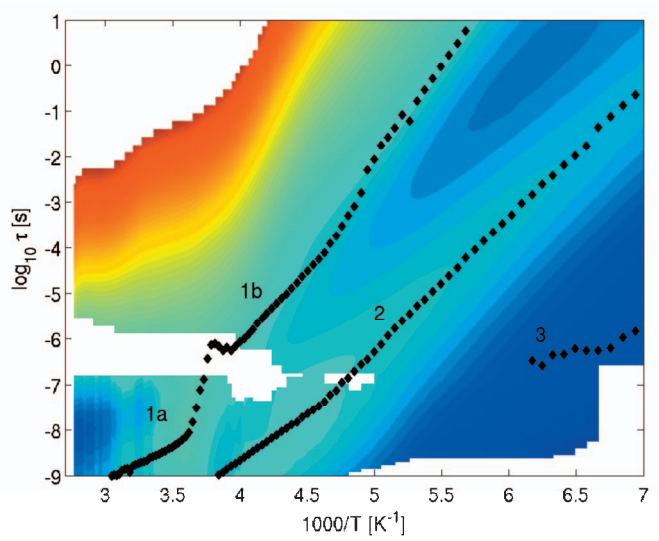

FIG. 3. (Color) Intensity plot of the experimental data as a function of $\tau=1/(2\pi f)$ and $1000/T$ for the n_8-sample. The black symbols represent the peak positions obtained from the curve fits with the labeling discussed in the text.

symmetric with $a=b$ in the range 0.3–0.4. The temperature dependence of the relaxation time is well described by an Arrhenius equation

$$\tau = \tau_0 \exp\left[\frac{E_a}{k_B T}\right], \tag{2}$$

with an activation energy, $E_a=56\pm3$ kJ/mol below 215 K. However, at this temperature we observe a change in the activation energy to $E_a=39$ kJ/mol at higher temperatures.

At these higher temperatures another process is observable that is marked 1b in Fig. 3. In the temperature region up to T'_m, also this process has approximately an Arrhenius behavior, with an activation energy, $E_a=49$ kJ/mol. Concerning the shape of the peak, the b-parameter is 0.3 up to 0.5 while the a-parameter is difficult to extract due to low frequency contributions. Around T'_m a dynamical transition occurs in that the temperature dependence becomes more pronounced. The overlap with low frequency contributions makes the data analysis in this region difficult, but the data suggest that the transition is due to a merging with another process, marked 1a in Fig. 3. Above T'_m the temperature dependence of this process is well described by the Vogel–Fulcher–Tammann (VFT) expression[40,41]

$$\tau = \tau_0 \exp\left[\frac{D_{\mathrm{VFT}} T_0}{T - T_0}\right], \tag{3}$$

with $D_{\mathrm{VFT}}=1.13$ and $T_0=253$ K.

Above 200 K the ionic conductivity dominates at low frequencies. At the highest temperatures the polarization effects due to charge buildup at the interfaces with the electrodes start to be prominent and hence these data are discarded. Moreover, in between the slow process and the ionic conductivity another process is observed that could be attributed to a relaxation process partly submerged into the ionic conductivity. However, the amplitude of this process is substantially larger than the other relaxation processes and the physical origin of this process is further discussed below.

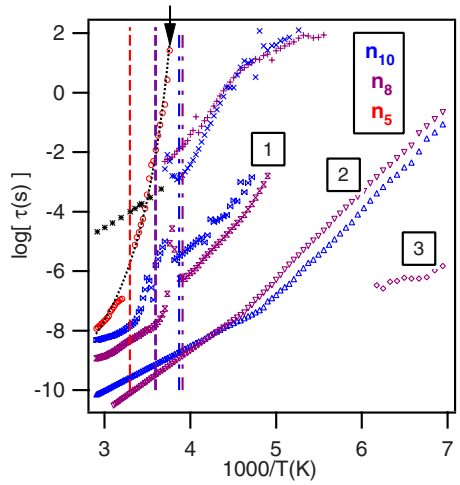

FIG. 4. (Color online) Arrhenius plot of the relaxation processes. The 1–processes are represented with circles (n_5), time glass (n_8), and tilted time-glass (n_{10}). The dotted line is a fit to the data for the 1a-process of sample n_5 using Eq. (3). Process 2 is represented with down triangles (n_8) and up triangles (n_{10}). Process 3 is marked with diamonds. Crosses represent the observed MW process, + and × for the n_8 and n_{10} samples, together with the estimation described in the text (∗). The vertical dashed lines are the T_m and the dashed-dotted lines the T'_m. The arrow marks the calorimetric glass transition for the low hydrated sample.

The n_{10}-sample has similar dynamical characteristics as the n_8-sample discussed above, as shown in Fig. 4. For process 2 we observe $E_a=56\pm3$ kJ/mol at low temperatures and $E_a=31$ kJ/mol above 210 K. Below T'_m τ_1 is approximately described by an Arrhenius law with $E_a=62$ kJ/mol. The behavior above T'_m is quite dramatic indicating a $D_{\mathrm{VFT}}<0.1$. However, a single VFT-expression does not describe all the data above T'_m satisfactorily.

For the sample hydrated at room humidity only the slow relaxation (process 1) can be reliably extracted, although there are indications of faster dynamics. The n_5-sample also has a pronounced step in the dielectric response around T_m, in accordance with a previous suggestion that the gel phase has a lower dielectric strength.[17] The step is also related to the change in thickness that occurs at the phase transition.

IV. DISCUSSION

A. Data analysis

Dielectric spectroscopy on a multicomponent structure requires careful analysis since the measured permittivity is not necessarily a simple superposition of the intrinsic contributions.[42] However, for planar dielectric media consisting of two components the measured permittivity $\varepsilon_{\mathrm{tot}}$ is

$$\varepsilon_{\mathrm{tot}} = \frac{1}{\frac{h_{\mathrm{H_2O}}}{h_{\mathrm{tot}}\varepsilon_{\mathrm{H_2O}}(\omega)} + \frac{h_{\mathrm{POPC}}}{h_{\mathrm{tot}}\varepsilon_{\mathrm{POPC}}(\omega)}}, \tag{4}$$

where $\varepsilon(\omega)$ and h are the permittivity and thickness of the respective layers.

The mathematical form of Eq. (4) results in a so-called Maxwell–Wagner (MW) peak, which has previously been observed in lipid systems.[14] It is important to emphasize that

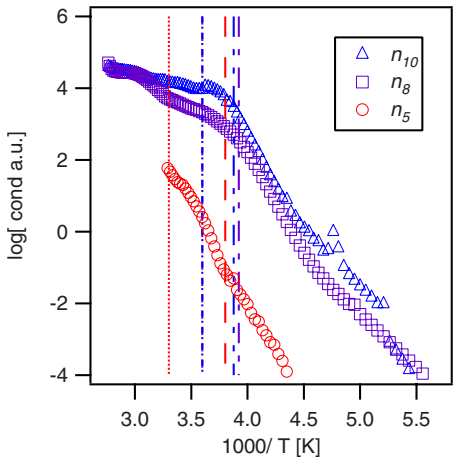

FIG. 5. (Color online) Temperature dependence of the ionic conductivity for n_5 (circles), n_8 (squares), and n_{10} (triangles). The transition temperature T_m are marked with vertical lines, dotted (n_5), dashed (n_8), and dashed-dotted (n_{10}). The transition temperature T'_m are marked with vertical lines long-dashed (n_5), long-dashed-dotted (n_8), and long-dashed-dotted-dotted (n_{10}).

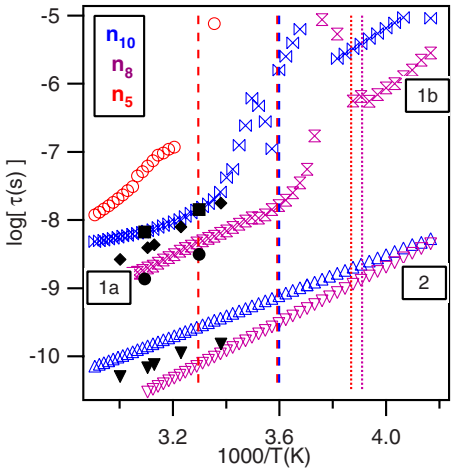

FIG. 6. (Color online) High temperature region of the Arrhenius plot with the same symbols as in Fig. 4. Also included are relaxation times obtained from literature data for the lipid process: NMR at n_w=8.2 ◆ (Ref. 5), head-group reorientation in DMPC from MD at n_w=5 ■ and n_w=10 ● (Ref. 25), and the water processes: NMR ▼ at n_w=8.2 (Ref. 5).

a MW peak is of purely static origin and not related to the reorientation of the dipoles in the system. The position of the MW-peak can be estimated using literature values for the thicknesses[33] and dielectric constants of the layers.[43] For the conductivity of the water in our system we use the conductivity of ultrapure water.[43] The conductivity of POPC is not known, but as long as it is lower than that of bulk water it only has a marginal effect on the MW-peak position. The estimated τ_{MW} is included in Fig. 4, that perfectly extrapolates to those observed for the process partly submerged in the conductivity. We therefore attribute this process to MW effects, which is also supported by the fact that the amplitude is substantially larger than other relaxation processes.

The mathematical form of Eq. (4) gives that the peak position, obtained from the straightforward superposition used in the data analysis is not necessarily the intrinsic peak position of the layers. The most important effects are that the relaxation strengths are significantly lower than in bulk and the intrinsic relaxation times may be shifted to slightly faster time scales.

B. Conductivity

Figure 5 shows the measured ionic conductivity as a function of hydration level, which reveals that the ionic conductivity is several orders of magnitude smaller without excess water. This implies that the ionic conductivity of the lipid indeed is small compared to bulk water. From Eq. (4) and assuming $\sigma_{H_2O}h_{POPC} \gg \sigma_{POPC}h_{H_2O}$ the total ionic conductivity is obtained as

$$\sigma = \frac{h_{tot}\sigma_{H_2O}\sigma_{POPC}}{\sigma_{H_2O}h_{POPC} + \sigma_{POPC}h_{H_2O}} \approx \frac{h_{tot}\sigma_{POPC}}{h_{POPC}}. \quad (5)$$

This shows that under present experimental conditions the measured conductivity is, to a good approximation, proportional to that of the lipid layers.

Figure 5 shows that for the n_5-sample the increase is systematic and gradual up to T_m, beyond which the low frequency data become very noisy. This is most probably induced by the change in thickness that accompanies the phase transition, which results in bad connections with the electrodes. The two hydrated samples have similar conductivity that is significantly higher than for the n_5-sample. Moreover, just above T'_m both samples show a transition to a significantly smaller temperature dependence. A similar transition has previously been observed for other lipid systems.[14] This emphasizes the link between structural arrangement of the lipids and the conductivity across the membrane. Computer simulations have shown that the rate limiting step of water permeability is the solvation in the dense tail region next to the lipid head-groups.[20]

C. Water dynamics

Water in confinement has been studied using many different confinement geometries, and our observations for processes 2 and 3 are in general agreement with the commonly observed relaxation processes.[29–31,44] Examining process 2 in some more detail we note that slightly above 210 K, which is close to the onset temperature T_h in the TMDSC-experiment for the n_{10}- and n_8-samples, there is a decrease in activation energy for process 2. This transition is particularly strong for the n_{10}-sample and results in that at high temperatures τ_2 is faster for n_8 than n_{10}. A plausible explanation for the latter is that for the n_8-sample the hydrogen bonded network is not fully developed and the water molecules interact primarily with the lipid heads. Further increasing the water content increases the number of water-water interactions such that the hydrogen bonded network becomes more important, which could slow down the dynamics. However, as discussed above, the layered geometry of the sample may cause a slight shift of the observed relaxation peak compared to the intrinsic relaxation process.

The high temperature dielectric data shown in Fig. 6 can be compared with previous experimental results and computer simulations. Included in Fig. 6 are relaxation times computed from diffusion constants of water and POPC in

TABLE II. Dielectric relaxation times for hydrated POPC multibilayers at 310 K. τ_1=lipid head and τ_2=water, $n_{\text{water/lipid}}$.

Relaxation	log τ (s)
$\tau_1(n_5)$	−5.94
$\tau_1(n_8)$	−8.46
$\tau_2(n_8)$	−10.25
$\tau_1(n_{10})$	−7.99
$\tau_2(n_{10})$	−9.69

multilamellar liposomes (n_w=8.2) obtained by pulse field gradient NMR.[5] The result can be compared with our data using the standard assumptions that $\tau=1/Dq^2$, dielectric experiments are performed at $q=1$ Å^{-1},[45] and the relaxation time $\tau_{\text{diel}}\sim 3\tau_{\text{NMR}}$.[46] Figure 6 shows that the NMR data agree fairly well with process 2 for the water dynamics. In Ref. 8 we compare the present water relaxation of the n_{10} sample also with QENS data on similar lipid systems. It is there shown that the relaxation times obtained with QENS at $q=1$ Å^{-1} are systematically faster than the dielectric relaxation times, probably due to the fact that the two experimental techniques probe different types of motions.

D. Lipid dynamics

In Fig. 6 the relaxation times for the phospholipid headgroup reorientation obtained from NMR experiments[5] and MD simulations[25] (calculated from diffusion constants, as given above for NMR data, but with $\tau_{\text{diel}}\sim\tau_{\text{MD}}$) are included, which agree well with our observations for process 1a. Hence, we attribute this process to lipid dynamics, which is also supported by the fact that this process remains observable even at very low hydration levels. Note that in dielectric spectroscopy the apolar acyl tails are practically invisible due to their low dielectric response, but MD simulations of 1,2-dimyristoyl-sn-glycero-3-phosphocholine (DMPC) show that the head-group relaxation time is somewhat faster than the relaxation time of the whole lipid.[25] Moreover, the pulse field gradient NMR data in Fig. 6 are for 2D lateral diffusion within the membrane. Hence, the dielectric experiment probes the planar lateral diffusion, in agreement with previous findings.[11]

An interesting observation is that process 1 is faster for the n_8-sample than for the n_{10}-sample, that is, the lipid dynamics does not continuously become faster with more water in the system. The reason for this finding may be that also the water relaxation is faster for the n_8-sample and the dynamics of the water and the lipids indeed are intimately coupled, i.e., the ratio τ_1/τ_2 is similar for the n_8 and the n_{10} samples at biological temperatures (see Table II).

Process 1a has a very pronounced temperature dependence. For n_5 the calorimetric glass transition T_g seems to be identical to T_m', since it also matches the dynamical glass transition, using the standard definition $T_g=T(\tau=100\ \text{s})$ (see Fig. 4). For the more hydrated samples no clear calorimetric T_g could be observed as discussed above in relation to the TMDSC data presented in Fig. 1. However, we note that process 1a becomes dramatically slower just above T_m' in close resemblance to the slowing down just above a glass transition. This implies that T_m' may play a similar role as for the n_5-sample. A theoretical treatment of the ripple phase also shows that a corrugated surface gives an anisotropic dielectric permittivity and a larger distribution of relaxation times.[17] We note that for all the hydration levels investigated here the dielectric loss peaks are smeared out around the main transition temperature. However, the typical average relaxation time remains similar above and below T_m. Our observations show that the major dynamical enhancement occurs upon going from the gel to the ripple phase. Around the ripple to liquid phase, where the most dramatic structural changes occur, the dynamics becomes more heterogeneous, as evident from the increased broadening of the relaxation peak. The reason for this may be that the membrane incorporates both ordered and disordered phases.

Below T_m' the temperature dependence of the observed lipid relaxation becomes less pronounced with a cross-over to an Arrhenius temperature dependence. Our analysis suggests that processes 1b and 1a indeed are two different processes, although the interference of other processes inhibits any definite statement. Thus our data looks very similar to the classical merging of the α- and β-relaxations in ordinary glasses with a transition temperature given by T_m'. We note that also the n_5-sample shows indications of a secondary process, but it is too weak to be reliably extracted.

E. General

Based on infrared experiments two transient microdomains of water adjacent to lipid membranes have been proposed: (i) a high density phase of water molecules interacting with the phosphate and carbonyl groups and (ii) a low density network water phase with a lower degree of ordering.[36] QENS experiments have provided support for two types of water dynamics: tightly bound rotational dynamics at picosecond time scale and, at elevated hydration levels, an only moderately slower quasi-free diffusion.[7] This is also in agreement with both NMR experiments[5] and MD simulations,[19] showing that the dynamics of even the deepest lying water molecules is less than a factor of 5 slower than for bulk water. This implies that the surface water and the more bulk-like water will in the dielectric spectra appear as a single broad relaxation process and not as two separate peaks. This supports our attribution of process 1b to motions of lipid head groups rather than to water.

The glass transition of hydrated POPC has also been explored by mechanical investigations, which reveal two relaxation processes.[27] The peak positions of these two processes agree very well with processes 1b and 2, respectively, observed in the present study. However, the authors attribute the high temperature process to the α-process of water, but, as described above, neither NMR, QENS, nor MD simulations provide any support for a water process several orders of magnitudes slower than the "universal" process of confined water.[29] Moreover, the Arrhenius behavior with a low activation energy and the lack of merging with the faster

water process give further arguments against the attribution of the mechanical high temperature process to an α-relaxation of water.

Thus, the general picture that emerges from our observation is that below T'_m the dynamics of the head groups is a local process of presumably reorientational character similar to the β-relaxation in a glass. Increasing the temperature major dynamical changes occur prior to the main phase transition. Above T'_m there is a dramatic speeding up of the lipid process and 2D translational diffusion becomes possible. Hence, in the biological active phase the lipids are much more mobile and exhibit more cooperative dynamics bearing resemblance with the α-relaxation in supercooled liquids. These more global motions have proven essential for the lipids role as host to proteins embedded in biological membranes. Since previous investigations have revealed that the chemistry of the head groups is the determining factor for the dynamics of phospholipids and the chain length dependence is less important,[11] the present findings bear promises of general validity for a larger range of lipid membranes.

V. CONCLUSIONS

We have shown that the structural relaxation processes of confined water and lipids can be extracted using dielectric spectroscopy on planar, lamellar membranes. We observe the two relaxation processes frequently reported for nanoconfined water. The experimental data show that the phospholipids have a complex dependence on temperature and hydration level. At high temperatures there is a non-Arrhenius behavior, while at lower temperatures there is, at least for high hydration levels, a transition, or bifurcation, to a process with an Arrhenius temperature dependence. This low temperature dynamics, which is attributed to the reorientation dynamics of the lipid head group, is very similar to the secondary relaxation process in ordinary glasses. However, the dynamical transition does not occur at the main phase transition. Instead, we show that the major dynamical changes occur at a pretransition of the membrane that is attributed to the gel to ripple transition. In this temperature region there is also a kink in the temperature dependence of the ionic conductivity.

ACKNOWLEDGMENTS

Financial support from the Swedish Natural Science Research Council is gratefully acknowledged.

[1] D. M. Engelman, Nature (London) **438**, 578 (2005).
[2] J. Milhaud, Biochim. Biophys. Acta **1663**, 19 (2004).
[3] R. Venable, Y. Zhang, B. Hardy, and R. Pastor, Science **262**, 223 (1993).
[4] T. M. Bayerl, Curr. Opin. Colloid Interface Sci. **5**, 232 (2000).
[5] H. C. Gaede and K. Gawrisch, Biophys. J. **85**, 1734 (2003).
[6] J. Fitter, R. Lechner, and N. Dencher, J. Phys. Chem. **103**, 8036 (1999).
[7] S. König, E. Sackmann, D. Richter, R. Zorn, C. Charlie, and T. M. Bayerl, J. Chem. Phys. **100**, 3307 (1994).
[8] J. Swenson, F. Kargl, P. Berntsen, and C. Svanberg, J. Chem. Phys. **129**, 045101 (2008).
[9] M. Hildenbrand and T. Bayerl, Biophys. J. **88**, 3360 (2005).
[10] M. Anotonietti, M. Neese, G. Blum, and F. Kremer, Langmuir **12**, 6636 (1996).
[11] A. Haibel, G. Nimtz, R. Pelster, and R. Jaggi, Phys. Rev. E **57**, 4838 (1998).
[12] B. Klögsen, C. Reichle, S. Kohlsmann, and K. Kramar, Biophys. J. **71**, 3521 (1996).
[13] R. Pottel, K.-D. Göpel, R. Henze, U. Kaatze, and V. Uhlendorf, Biophys. Chem. **19**, 233 (1984).
[14] J. Cooper and R. Hill, J. Colloid Interface Sci. **180**, 27 (1996).
[15] M. Tirado, C. Grosse, W. Schrader, and U. Kaatze, J. Non-Cryst. Solids **305**, 373 (2002).
[16] A. Enders and G. Nimtz, Ber. Bunsenges. Phys. Chem **88**, 512 (1984).
[17] A. Raudino, F. Castelli, G. Briganti, and C. Cametti, J. Chem. Phys. **115**, 8238 (2001).
[18] P. Berntsen, R. Bergman, H. Jansson, M. Weik, and J. Swenson, Biophys. J. **89**, 3120 (2005).
[19] T. Rog, K. Murzyn, and M. Pasenkiewicz-Gierula, Chem. Phys. Lett. **352**, 323 (2002).
[20] D. Tieleman, S. Marrink, and H. Berendsen, Biochim. Biophys. Acta **1331**, 235 (1997).
[21] K. Sengupta, V. Raghunathan, and J. Katsaras, Phys. Rev. E **68**, 031710 (2003).
[22] H. Binder and K. Gawrisch, Biophys. J. **81**, 969 (2001).
[23] M.-C. Bellissent-Funel, J. Mol. Liq. **84**, 39 (2000).
[24] V. Volkov, D. Palmer, and R. Righini, Phys. Rev. Lett. **99**, 078302 (2007).
[25] C.-J. Högberg and A. Lyubartsev, J. Phys. Chem. B **110**, 14326 (2006).
[26] E. Shalaev and P. Steponkus, J. Phys. Chem. **107**, 8734 (2003).
[27] C. Castellano, J. Generosi, A. Congiu, and R. Cantelli, Appl. Phys. Lett. **89**, 233905 (2006).
[28] R. Bergman and J. Swenson, Nature (London) **403**, 283 (2000).
[29] S. Cerveny, G. A. Schwartz, R. Bergman, and J. Swenson, Phys. Rev. Lett. **93**, 245702 (2004).
[30] J. Swenson, H. Jansson, and R. Bergman, Phys. Rev. Lett. **96**, 247802 (2006).
[31] J. Swenson, H. Jansson, W. S. Howells, and S. Longeville, J. Chem. Phys. **122**, 084505 (2005).
[32] C. Angell, Science **319**, 582 (2008).
[33] S. Leekumjorn and A. Sum, J. Phys. Chem. B **111**, 6026 (2007).
[34] M. Seul and M. Sammon, Thin Solid Films **185**, 287 (1990).
[35] H. Binder, B. Kohlstrunk, and H. Heerklotz, J. Colloid Interface Sci. **220**, 235 (1999).
[36] H. Binder, Eur. Biophys. J. **36**, 265 (2007).
[37] E. Verdonck, K. Schaap, and L. Thomas, Int. J. Pharm. **192**, 3 (1999).
[38] C. Hsieh and W. Wu, Biophys. J. **71**, 3278 (1996).
[39] R. Bergman, J. Appl. Phys. **88**, 1356 (2000).
[40] C. A. Angell, Science **267**, 1924 (1995).
[41] M. D. Ediger, C. A. Angell, and S. R. Nagel, J. Phys. Chem. **100**, 13200 (1996).
[42] R. Pelster, Phys. Rev. B **59**, 9214 (1999).
[43] *Handbook of Chemistry and Physics* (CRC, Boca Raton, FL, 2007).
[44] J. Swenson, H. Jansson, J. Hedström, and R. Bergman, J. Phys.: Condens. Matter **19**, 205109 (2007).
[45] A. Arbe, A. Alegria, J. Colmonero, S. Hoffman, L. Willner, and D. Richter, Macromolecules **32**, 7572 (1999).
[46] A. Volmari and H. Weingärtner, J. Mol. Liq. **98–99**, 295 (2002).